PLANT SCIENCE TODAY
Vol 12(3): 1-14
https://doi.org/10.14719/pst.9740

eISSN 2348-1900

RESEARCH ARTICLE

# Green synthesis of silver nanoparticles (AgNPs) with *Hypericum wightianum* : Characterization and evaluation of its antibacterial activity, antioxidant activity and toxicity assessment on *Artemia salina*

**Neethu Vijayakumar[1*], Sumitha V R[2], A Gangaprasad[3] & S Muthukrishnan[3]**

[1]Department of Botany, Mahatma Gandhi College, Kesavadasapuram, Thiruvananthapuram 685 004, Kerala, India
[2]Department of Botany, NSS College Pandalam, Pathanamthitta 689 501, Kerala, India
[3]Department of Botany, University of Kerala, Kariavattom, Thiruvananthapuram 695 581, Kerala, India

*Correspondence email - neethusmithan06@gmail.com

Received: 31 May 2025; Accepted: 29 July 2025; Available online: Version 1.0: 19 August 2025; Version 2.0: 22 August 2025

**Cite this article:** Neethu V, Sumitha VR, Gangaprasad A, Muthukrishnan S. Green synthesis of silver nanoparticles (AgNPs) with *Hypericum wightianum* : Characterization and evaluation of its antibacterial activity, antioxidant activity and toxicity assessment on *Artemia salina*. Plant Science Today. 2025; 12(3): 1-14. https://doi.org/10.14719/pst.9740

## Abstract

In the present study, *in vitro H. wightianum* plant extract was used for the phytosynthesis of AgNPs. It was observed that the reduction of aqueous silver ions ($Ag^+$) to AgNPs was facilitated by the extract, resulting in the formation of stable AgNPs. The synthesized AgNPs were characterized through various spectroscopic and microscopic analyses. The nanoparticles showed a sharp absorbance peak at 480 nm on UV-Vis spectroscopy. Fourier Transform Infrared Spectroscopy (FTIR) confirms the presence of flavonol, glycosides and phloroglucinols. X-ray diffraction (XRD) was used to characterize the reduction of silver ions to silver element. It shows the different distinct peaks at 25.78 °, 39.41 °, 41.37 ° and 76.26 ° correspond to the (0 1 2), (1 1 1), (1 0 1) and (3 1 1) planes of standard XRD peak reflections of silver crystal. The formation of monodispersed low polydispersity nanoparticles (16.47 nm) was revealed by the transmission electron micrograph (TEM) and energy-dispersive X-ray spectroscopy (EDX) analysis confirms the presence of elemental silver. AgNPs showed good antioxidant properties in DPPH (2, 2-diphenyl-1-picrylhydrazyl), hydrogen peroxide ($H_2O_2$), nitric oxide (NO) radical scavenging and ferric reducing power assays. This result proved that AgNPs have strong antioxidant activity, which is comparable to the standard. Antioxidant activity of AgNPs increased dose-dependently, based on the reduction of electron or hydrogen acceptors. Antibacterial activity of AgNPs was demonstrated against test strains, showing significant inhibition. A maximum zone of inhibition of 15 mm was observed against *Staphylococcus aureus,* followed by 14 mm against *Pseudomonas aeruginosa* at 80 µg/mL concentration. The AgNPs showed moderate toxicity against *A. salina*. The present study demonstrates the potential of *in vitro H. wightianum* extract for the phytosynthesis of AgNPs with antioxidant, antibacterial and moderate toxicity properties.

**Keywords:** antibacterial activity; antioxidant activity; *Artemia salina*; ecotoxicity; *Hypericum wightianum;* silver nanoparticles

## Introduction

In recent decades, studies on the green synthesis of nanoparticles have increased due to innovative applications in various biological and medicinal industries. Nanoparticles have paved the way for the development of novel materials by offering new avenues for design and property assessment. By precisely controlling the size, shape and molecular distribution of nanoparticles, researchers can tailor their properties to suit specific applications (1). AgNPs have emerged as promising material due to their distinctive properties. One of the primary advantages of nanoparticles lies in their exceptionally large surface area relative to their tiny size, facilitating increased reactivity and interactions with other molecules. These remarkable properties have earned these metal nanoparticles great interest in the 21st century. Nanotechnology is an emerging technology that involves manipulating matter at the nanoscale or atomic level and has incredible applications in drug delivery (2), cancer diagnosis (3, 4), bacterial diseases, in agriculture, detecting and controlling diseases and pests (5), environmental sensors (6), quantum computing and artificial intelligence (7). Besides, it can be used to create superior household products such as degreasers, stain removers and self-cleaning paints and lead to highly precise as well as efficient manufacturing processes (8, 9). Developing and experimenting with new nanoparticles and investigating their properties for human welfare are the major interests. Researching and innovating new nanoparticles, along with their possible applications for the benefit of humanity, constitutes the primary focus of interest.

Green nanotechnology has garnered significant

attention due to its eco-friendly and cost-effective synthesis of nanoparticles, eliminating harmful reagents. Noble metal nanoparticles, especially AgNPs, have unique physicochemical properties, that are significant for medical industries and for the development of innovative, new sustainable materials for defense applications (10, 11). Notably, AgNPs demonstrate exceptional antimicrobial and antioxidant efficacy (12). So, recent research has been explored in the application of AgNPs in combating microbial infections and preventing bacterial growth, particularly in the context of antibiotic resistance (3). Traditionally, physical and chemical synthesis methods possess environmental concerns due to toxic substances and harmful by-products (4). However, green synthesis of nanoparticles using microorganisms and plant extracts provides an eco-friendly and cleaner alternative. While microorganism-based synthesis presents challenges, plant-mediated synthesis offers advantages, including low-cost, non-toxic and eco-friendly by-products (13). Due to these properties, plant extracts serve as effective reducing and capping agents, yielding stable AgNPs with diverse shapes and dimensions, thereby enhancing synthesis efficiency. Recently, many medicinal and ornamental plants have been used for the synthesis of AgNPs, such as *Ceropegia thwaitesii* (12), *Helicteres isora* (3), *Psophocarpus tetragonolobus* (14) and *Dianthus chinensis* (13).

In this research paper, we concentrate our attention on the green synthesis of AgNPs using *in vitro* raised *H. wightianum* plant extract and analysis of their antioxidant and antibacterial activity against human pathogens. Furthermore, the toxic effects of AgNPs on the mortality of *A. salina* are assessed and discussed. In essence, toxicity studies are an integral part of the green synthesis process, providing crucial information for ensuring the safety and responsible application of AgNPs. *A. salina* is a primitive aquatic arthropod (salt lakes) of the Artemiidae family, which is more closely related to Triops and Cladocerans than to true shrimp from hypersaline ecosystems. The United States Environmental Protection Agency (US-EPA) has approved *A. salina* as one of the test organisms for acute toxicity testing (15). *Artemia* is one of the most valuable model test organisms available for ecotoxicity testing of many nanoparticles (3, 4). Toxicity studies also help to assess the potential environmental impact of AgNPs nanoparticles, including their effects on aquatic and terrestrial organisms. This is crucial for ensuring that green synthesis methods are truly sustainable and do not pose unintended risks to the environment.

## Materials and Methods

### Sample preparation

*H. wightianum* was collected from Pamparpuram, Kodaikanal in the region of Western Ghats of Tamil Nadu, India, in July 2019. The collected plant was identified and confirmed by the plant taxonomist Dr. Seeni Sooriamuthu, School of Biosciences, Mar Athanasios College for Advanced Studies, Tiruvalla. The voucher specimens were prepared and submitted to the Department of Botany herbarium, University of Kerala, Thiruvananthapuram, Kerala and authenticated (Voucher/Accession No. KUBH11410). These plants were cultured *in vitro* in the plant tissue culture laboratory. Plant materials were collected from *in vitro* raised plants and washed with sterile Milli-Q water. The plant was then crushed using a mortar and pestle. The plant extracts were prepared, then the extract was filtered with Whatman No. 1 filter paper and the extract was stored in a refrigerator for further use (12).

### Synthesis of AgNPs

The AgNPs synthesis was carried out following the methodology established (3). The plant extracts were used for the AgNPs synthesis. 90 mL of 1 mM aqueous silver nitrate ($AgNO_3$) (Himedia) solution was added to 10 mL of the extract, in 250 mL conical flasks and kept at 30 $^0$C in a shaker for 24 hr. After incubation, the experimental mixture (plant extract and silver nitrate) was centrifuged at 15000 rpm for 20 to 25 min. The by-product mixture was then washed using Milli-Q water. This process was conducted after each centrifugation; the colloidal pellet obtained was poured into a Petri dish and dried by placing it in a sterile chamber inside the culture room. After drying, the powder was transferred to an Eppendorf tube, sealed with paraffin wax film and placed in a refrigerator for further work.

### UV-Visible spectra

The biosynthesized AgNPs in the bio-reduction process of silver ions in solutions was checked using the UV-vis spectrum in (UV-1700 pharma spec, Shimadzu, Japan). The measurements were done on a wavelength scale of 200 to 800 nm, achieving a resolution of 1 nm and with a generation time of 1 sec with Malvern software. Measurements were taken at different time intervals over a period of 24 hr.

### FE-SEM EDX analysis

Field Emission-Scanning Electron Microscopic (FE-SEM) analysis was conducted using the TESCAN-3236741 instrument at an accelerating voltage of 10 Kv. Sample preparation involved placing a small amount of the sample on a carbon-coated copper grid, removing excess solution with blotting paper and drying the film under a mercury lamp for 5 min (12). The elemental composition of the AgNPs was determined by EDX analysis; the dried AgNPs were drop-coated onto a carbon film and the EDX analysis was performed using the Oxford XMXN connected with the FE-SEM instrument (MAIA3 XMH).

### XRD analysis

The plant extracts with AgNPs were freeze-dried and ground for XRD analysis. The diffracted intensities for AgNPs were measured from 10 to 90 degrees at 2θ angles (3). The size of the biosynthesized AgNPs was calculated by the Debye-Scherrer formula;

$$D = \frac{K\lambda}{\beta cos\theta}$$

Where; K = Shape factor; λ = X-ray wavelength; β = Half the maximum intensity (FWHM) in radians and θ = Bragg's angle.

### FTIR analysis

For FTIR analysis, the AgNPs solution was centrifuged at 15000 rpm for 30 min and samples were allowed to read to Thermo Scientific Nicolet iS50 with KBr optics and a DTGS detector. The pellet was washed two to three times with 10 mL of Milli-Q water to clear out the free proteins/enzymes that were not capped during the biosynthesis of AgNPs (13). The particles and dry

plant powder were dried and ground with KBr separately and analyzed in a Thermo Scientific Nicolet Is50 to identify the biomolecules in plant extracts and those associated with bio-synthesized AgNPs.

## Transmission Electron Microscopy (TEM)

The size and morphology of biosynthesized AgNPs were determined by TEM analysis. For TEM analysis, dilute 25 µL of colloidal AgNPs solution with 0.5 mL Millipore Milli-Q water and sonicate the mixture using an ultrasonic bath and filtered with a 0.22 µm filter (Rankem Faridabad, India). Place a drop of the filtered solution on a Cu grid and allowed to dry under vacuum. Then, AgNPs were visualized using TEM and measurements were done by using NanoLab Inc., Waltham, MA, at 200 kV.

## *In vitro* antioxidant assays

### DPPH free radical scavenging assay

DPPH free radical scavenging potential of the AgNPs was determined (16) with modification. Various concentrations (10, 20, 30, 40, 50, 70, 90 and 100 µg/mL) of biosynthesized AgNPs and standard antioxidant butylated hydroxytoluene (BHT) were used for assaying scavenging activities. To the above samples, 1 mL of freshly prepared DPPH solution (1 mM) was added and subjected to thorough mixing on a vortex mixer. After that, it was incubated for 30 min in the dark. The absorbance of stable DPPH was then measured at 517 nm, with a control DPPH sample (without any sample) for comparison. Free radical scavenging activity was expressed as the percentage of inhibition that was calculated using the following equation;

$$\text{DPPH radical scavenging activity (\%)} = \frac{Ac - As}{Ac} X100 \,. \quad \text{(Eqn. 1)}$$

Here, Ac-control absorbance of DPPH radical + methanol, As sample absorbance of DPPH radical + AgNPs sample/standard BHT.

### $H_2O_2$ scavenging assay

$H_2O_2$ scavenging activity was analyzed (17) with slight modification. For the analysis, various concentrations (10, 20, 30, 40, 50, 70, 90 and 100µg/mL) of biosynthesized AgNPs and the control ascorbic acid were mixed with 50 µL of 5 mM $H_2O_2$ solution (HiMedia Laboratories, USA). The mixture was incubated for 30 min at room temperature and the absorbance was measured at 610 nm. The $H_2O_2$ scavenging activity percentage was calculated using Eqn. (1) .

### NO radical scavenging assay

NO radicals produced from sodium nitroprusside in aqueous solution at physiological pH react with oxygen to form nitrite ions. These ions were quantified using the modified Griess reaction reagent (18). In this study, NO radicals were produced from 100 µL of 20 mM sodium nitroprusside (HiMedia Laboratories, USA). These radicals were then incubated with 100 µL of AgNPs at varying concentrations (10, 20, 30, 40, 50, 70, 90 and 100 µg/mL) and were kept at room temperature for 60 min. BHT and a NO. scavenger served as positive controls. The percentage of NO radical scavenging activity was measured by Eqn. (1).

### Ferric Reducing Power Assay

The reducing power activity was analyzed (19) with slight modification. In this study, several concentrations of AgNPs solutions 10, 20, 30, 40, 50, 70, 90 and 100 µg/mL were combined with 2.5 mL of a 200 mM phosphate buffer at pH 6.6 and 2.5 mL of 1 % potassium ferricyanide. The mixture was incubated at 50 °C for 20 min and then cooled rapidly. Afterward, 2.5 mL of 10 % trichloroacetic acid (TCA) was added and immediately centrifuged at 3000 rpm for 8 min at room temperature. After centrifugation supernatant was mixed with the same amount of Milli-Q water. Then, 1 mL of 0.1 % ferric chloride solution was added to the upper layer and absorbance was immediately measured using a spectrophotometer (UV-1700 pharma spec, Shimadzu, Japan) at a wavelength of 700 nm. The results were then compared with those of BHT, which was used as positive control in the experiment. The reducing power percentage was calculated by Eqn. (1).

## Microorganisms

The antibacterial properties of AgNPs synthesized from *in vitro* raised plants of *H. wightianum* were evaluated against *Escherichia coli, Vibrio cholerae, S. aureus, P. aeruginosa, Mycobacterium, Salmonella typhi, Bacillus subtilis, Micrococcus luteus* and *Proteus mirabilis.*

## Antibacterial activity study

The assessment of the antibacterial activity of AgNPs was measured using the well diffusion method (20). The bacterial cultures were incubated overnight and then inoculated by evenly spreading them over freshly prepared nutrient broth plates. 100 µL of 24 hr old bacterial culture was swabbed (sterile cotton swabs) on the solidified broth plates. Wells were made by a well cutter and 35 µL of different concentrations of the AgNPs (20, 40 and 80 µg/mL) were loaded into the wells. Gentamicin (reference) was also loaded in one of the wells, allowed to incubate at 37 °C for 24 hr and the zone of inhibition was measured.

## Brine shrimp ecotoxicity assay

The brine shrimp (*A. salina*) assay was performed (4). Using a micropipette, the hatched cysts were collected and washed with cold water through a Millipore cellulose filter. Approximately 3 mg of cysts were incubated in 1000 mL of seawater in a conical flask under aseptic laboratory conditions (26 ± 2 °C). Proper aeration was maintained using a fish tank air pump. A 1000 µL solution containing the hatched nauplii and adults ~3 mg was taken using a micropipette. It was then transferred into a clean 6 -well plate and counted manually (21).

## Exposure study

An exposure study was conducted on both nauplii and adult brine shrimp (*A. salina*) for up to 72 hr, following the OECD testing guidelines (22). Various test concentrations (20, 40, 60, 80, 100, 125 and 150 µg/mL) of AgNPs were added to different cultures and the control culture was maintained without AgNPs. In a conical flask 100 mL of seawater with both nauplii and adults was exposed to cultures, with proper aeration using an aquarium air pump connected using long plastic pipes provided up to the bottom to prevent AgNP settling. The experimental conditions were maintained at an initial pH of 8.1, increasing to 8.4, with a 16:8 hr light cycle and a temperature of 26 ± 2 °C, during the entire experiment. No food was provided to the test organisms during the experimental period. The mortality percentages and $LC_{50}$ value were recorded at varying exposure periods and AgNPs concentrations were noted. Each experiment

was conducted in triplicate alongside the control and the % of mortality rate was calculated using the following formula:

$$\text{Mortality \%} = \frac{\text{No.of dead nauplii/adults}}{\text{initial No.of live nauplii/adult}} X100 \quad \text{(Eqn. 2)}$$

## Results and Discussions

The characterization of nanoparticles is based on their size and shape, surface area and disparity; these homogeneity properties play a key role in many applications (23). The understanding and management of nanoparticle synthesis and their applications are significant. The characterization of green-synthesized nanoparticles is achieved using various techniques, including UV-Visible, FE-SEM, XRD, FTIR and TEM (4, 13, 14). When the plant extract was combined with $AgNO_3$ solution and kept at room temperature, colour change occurred within an hour. The colour changed from pale yellow to dark brown as shown in (Fig. 1a-c) and this transformation shows the formation of AgNPs. The green synthesis method is efficient and rapid, which was well documented by several researchers who have worked with different plant systems (3, 12). The colour change was due to the excitation of surface plasmon vibrations during the reaction of plant extract with $AgNO_3$ (24). Silver is known as a good antimicrobial agent against various pathogens. It has good antioxidant potential also. Due to these properties, nowadays, researchers pay more attention to the green synthesis of AgNPs using different plant parts.

### UV-Visible spectra

UV-Visible absorption spectroscopy is a valuable technique for monitoring the reduction of silver ions ($Ag^+$) into neutral silver atoms ($Ag^0$) during the biosynthesis of AgNPs using plant extracts. The presence of surface plasmon resonance (SPR) in AgNPs is evident from the absorption band between 450-500 nm (25). Specifically, our UV-Vis analysis revealed a distinct absorbance peak at 480 nm (Fig. 1c), indicating protein-ligand complex formation and structural changes in proteins (26). The bioreduction of AgNPs from aqueous $AgNO_3$ solution was indirectly examined using UV-Vis spectroscopy (Fig. 1a & b). The SPR peak formation depends on several factors like the formation of particles, size, structure and shape of the nanoparticles (27, 28). Two or additional SPR bands correspond to the anisotropic molecules, whereas a single SPR band resembles the spherical form of nanoparticles. Notably, current biosynthesized AgNPs showed a spherical nature because single SPR bands were exhibited in the spectrum. The presence of flavone derivatives, hyperwightin B and benzophenone glycosides in *H. wightianum* plant extract likely plays a crucial role in reducing and stabilizing biosynthesized AgNPs.

### FTIR spectral analysis

Fig. 2 shows the FTIR spectrum of the synthesized AgNPs. It reveals the probable biomolecules existing in the plant extract, which are responsible for the bioreduction of silver ions and their interface with the synthesized AgNPs. The absorbance band analysis in bio-reduction was observed in the region of 500 - 4000 $cm^{-1}$. The IR band of AgNPs showed intense bands at 3330.15 $cm^{-1}$, 2930.23 $cm^{-1}$, 2359.69 $cm^{-1}$, 1605.15 $cm^{-1}$, 1380.15 $cm^{-1}$ and 1020.98 $cm^{-1}$ (Fig. 2a). The IR band of plant extract showed intense bands at 3339.65 $cm^{-1}$, 2949.03 $cm^{-1}$, 1675.35 $cm^{-1}$ and 1415.85 $cm^{-1}$ (Fig. 2b) and significant variance was observed among the spectral positions of the IR bands in plant extract and AgNPs due to the reduction process. The broad band at 3330.15 $cm^{-1}$ corresponds to the strong stretching vibrations of the hydroxyl group (-OH) of steroid sapogenin; this broad band was reduced from the extract of the 3339.65 $cm^{-1}$ spectrum. The broad band at 2930.23 $cm^{-1}$ corresponds to the broad strong stretching of amine salt N-H stretching; this broad band was reduced from extract of 2949.03 $cm^{-1}$ spectrum. The sharp two pronounced peaks observed at 1605.15 $cm^{-1}$ and 1380.15 $cm^{-1}$ can indicate the C=H and C=C stretching vibrations, which suggests the presence of alcohol and alkene groups within the plant extract that may play a role in the reduction process (29). Additionally, the IR band of plant extract exhibited a significant band at 1675.35 $cm^{-1}$ associated with the (C=C) stretching mode and $NH_2$ scissoring (1°-amines)

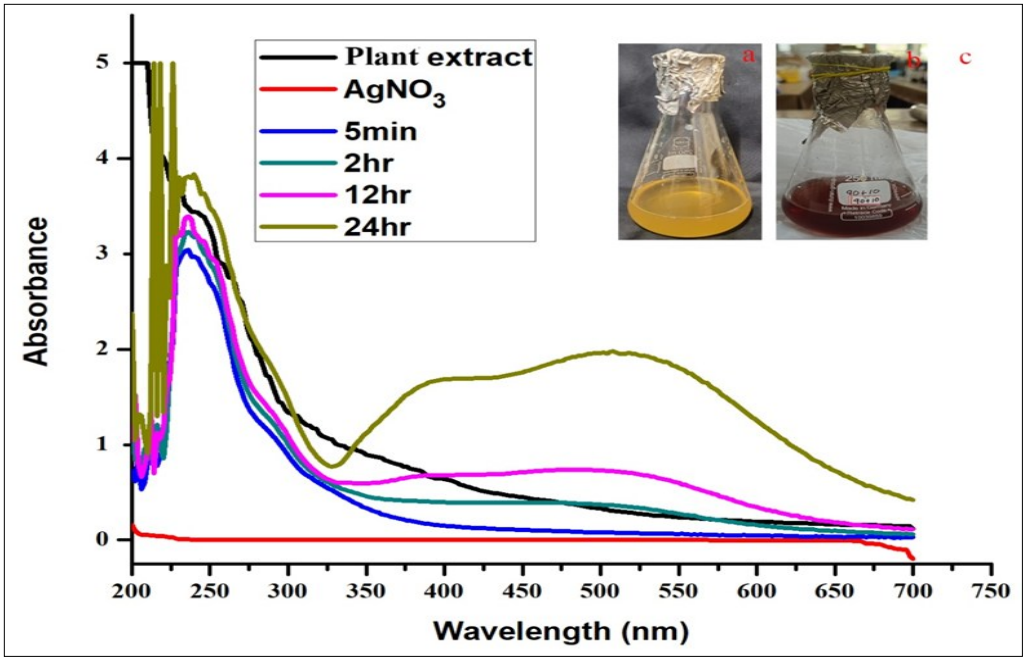


**Fig. 1.** UV-Visible spectra of biosynthesized AgNPs using *in vitro* raised plant extract. (a): extract; (b): colour changed after adding $AgNo_3$; (c): different time interval.

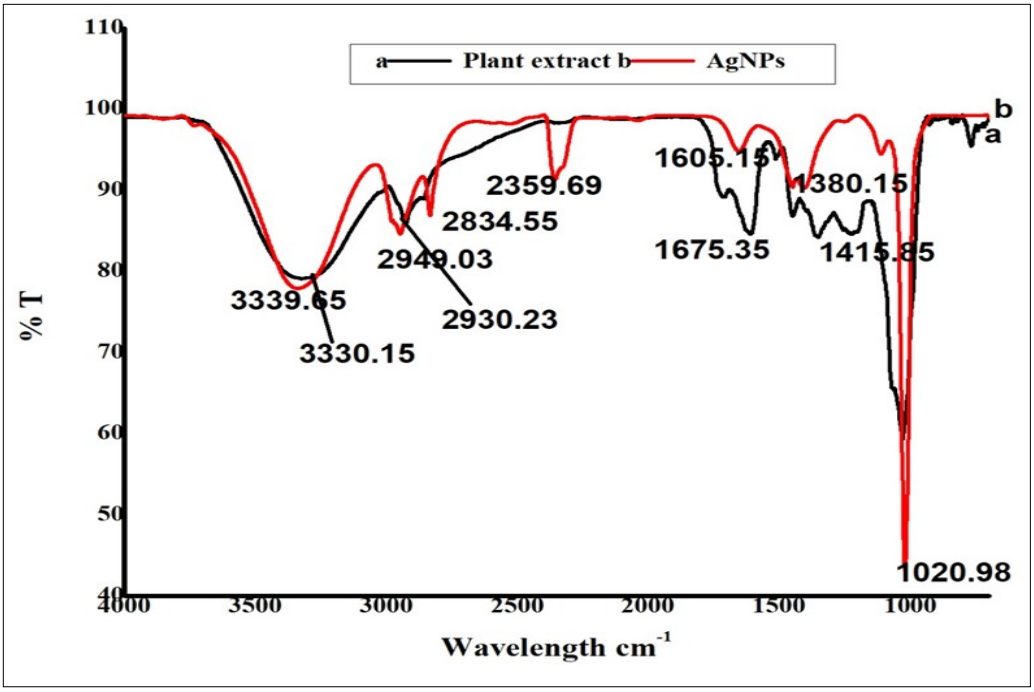


**Fig. 2.** FTIR analysis: (a) plant extract; (b) biosynthesized AgNPs.

groups from primary amines and this peak shifted to 1605.15 $cm^{-1}$,suggesting the potential interaction of these above-mentioned functional groups in AgNPs synthesis. This amine band indicates that hyperwightin derivatives can bind to $Ag^{+}$ through alcohol and alkene groups (30). The major peaks at 2930.23 $cm^{-1}$ and 2359.69 $cm^{-1}$ could be assigned to the C H stretching vibrations of methyl, methylene and methoxy groups (31). The mechanism of adsorption and capping of AgNPs by *H. wightianum* can be explained through the coordination of the carbonyl bond (1020.98 $cm^{-1}$), therefore, electron transfer from C O to biosynthesized AgNPs (32). This result suggests that hyperwightin derivatives are related to the AgNPs and also their secondary metabolite structures were not changed during the reaction with silver ions or after binding with AgNPs.

## XRD

The XRD pattern of biosynthesized AgNPs using the plant extract is shown in Fig. 3. The different distinct peaks at 25.78°, 39.41°, 41.37° and 76.26° correspond to the (0 1 2), (1 1 1), (1 0 1) and (3 1 1) planes of standard XRD peak reflections of silver crystal. This structural pattern also confirms and represents the spherical crystalline structure of AgNPs. The sharp peaks in the XRD pattern confirm the nature of biosynthesized AgNPs, aligning with previous reports (34, 35, 36). The average size of the biosynthesized AgNPs was calculated using the Debye-Scherrer formula to be 14.20 nm, which was slightly smaller than the average particle size determined by TEM analysis.

## FE-SEM with EDX analysis

The morphology and particle size of bio-synthesized AgNPs were

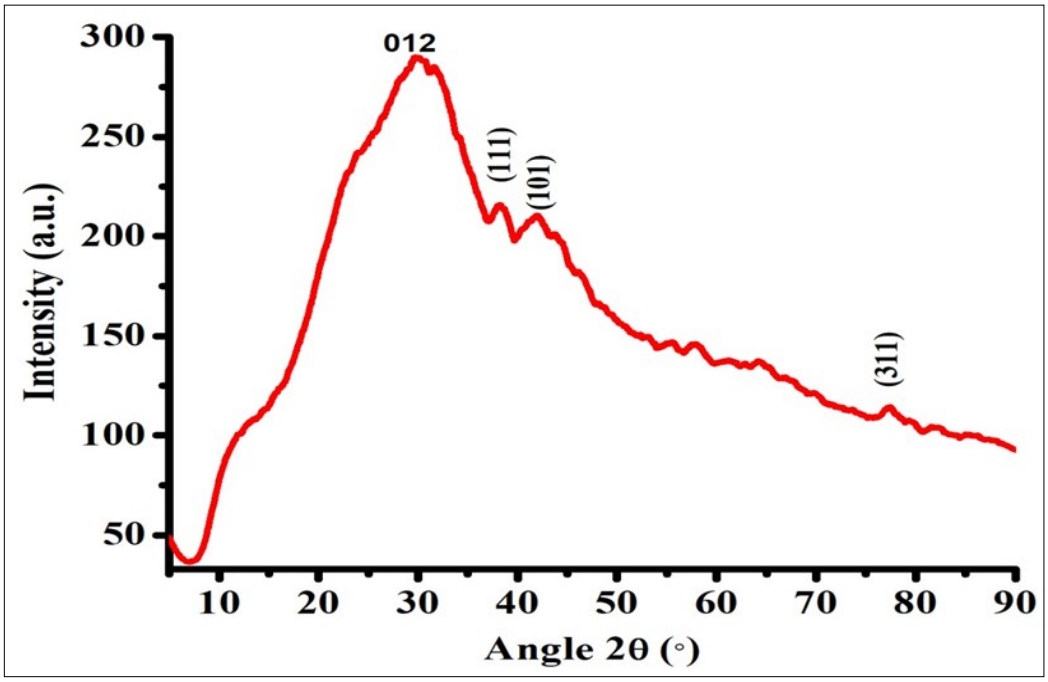


**Fig. 3.** XRD pattern of biosynthesized silver nanoparticles using plant extract. The planes (0 1 2), (1 1 1), (1 0 1) and (3 1 1) correspond to the standard XRD of silver crystal.

investigated by utilizing FE-SEM. FE-SEM analysis provide and revealed that the synthesized AgNPs exhibited rocky surface morphology with a diameter ranging from 30 to 40 nm. (Fig. 4a & b). The FE-SEM images of AgNPs suggest the joining of mono-dispersed AgNPs of high thickness. The previous study (12) reported that the diameter of the spherical AgNPs during synthesis with *C. thwaitesii* varied from 80 to 100 nm. When *Eucalyptus globulus* leaf broth was used yielded results varied, 70 to 100 nm (37). Higher magnification of FE-SEM images shows the surfaces of the deposited AgNPs clearly. The elemental composition and purity of elemental silver is typically identified by the EDX analysis, which shows the conservation of silver ions to elemental silver within the reaction mixture. The EDX spectrum (Fig. 4c) shows prominent metallic Ag signals. It is clear from the data obtained by EDX that silver content in percentage terms was 79.2 % with chlorine and carbon accounting 1.5 % and 6.4 % respectively (Fig. 4d). The presence of other signals, such as chlorine and carbon were also detected, suggesting the presence of organic moieties derived from plant extract used in the synthesis process. These organic molecules act as capping agents, stabilizing the nanoparticles and preventing aggregation. The presence of chlorine indicates that these organic moieties contain chloride groups, which function as capping agents. These findings demonstrate a phytochemical-mediated synthesis pathway, where plant extracts play a dual role in reducing silver ions into nanoparticles and capping them for enhanced stability. The most dominant sharp signal in the range 2.5 - 3.5 keV is for silver, which is distinctive for the absorption of crystalline AgNPs (3). Similar findings were reported by a recent study (13) for AgNPs synthesis using *Dianthus chinensis* that observed individual spherical-shaped AgNPs in the 2 - 4 keV range. Another study (12) also reported individual spherical-shaped AgNPs obtained at 3 keV using *C. thwaitesii.*

## TEM-SAED study

TEM images of individual biosynthesized AgNPs and their aggregates are shown in Fig. 5a-f. The images reveal that AgNPs were predominantly spherical and majority of the particles ranged from 10-100 nm (Fig. 5f). The average size of the crystalline AgNPs was determined to be 16.47 nm in diameter. Most of the particles were spherical in shape, with a tendency to mostly aggregate. However, individual particles were also present. The biomolecular coating on the surface layer of AgNPs is visible in Fig. 5c. This surface coating, comprising biomolecules of the plant extract, contributes to

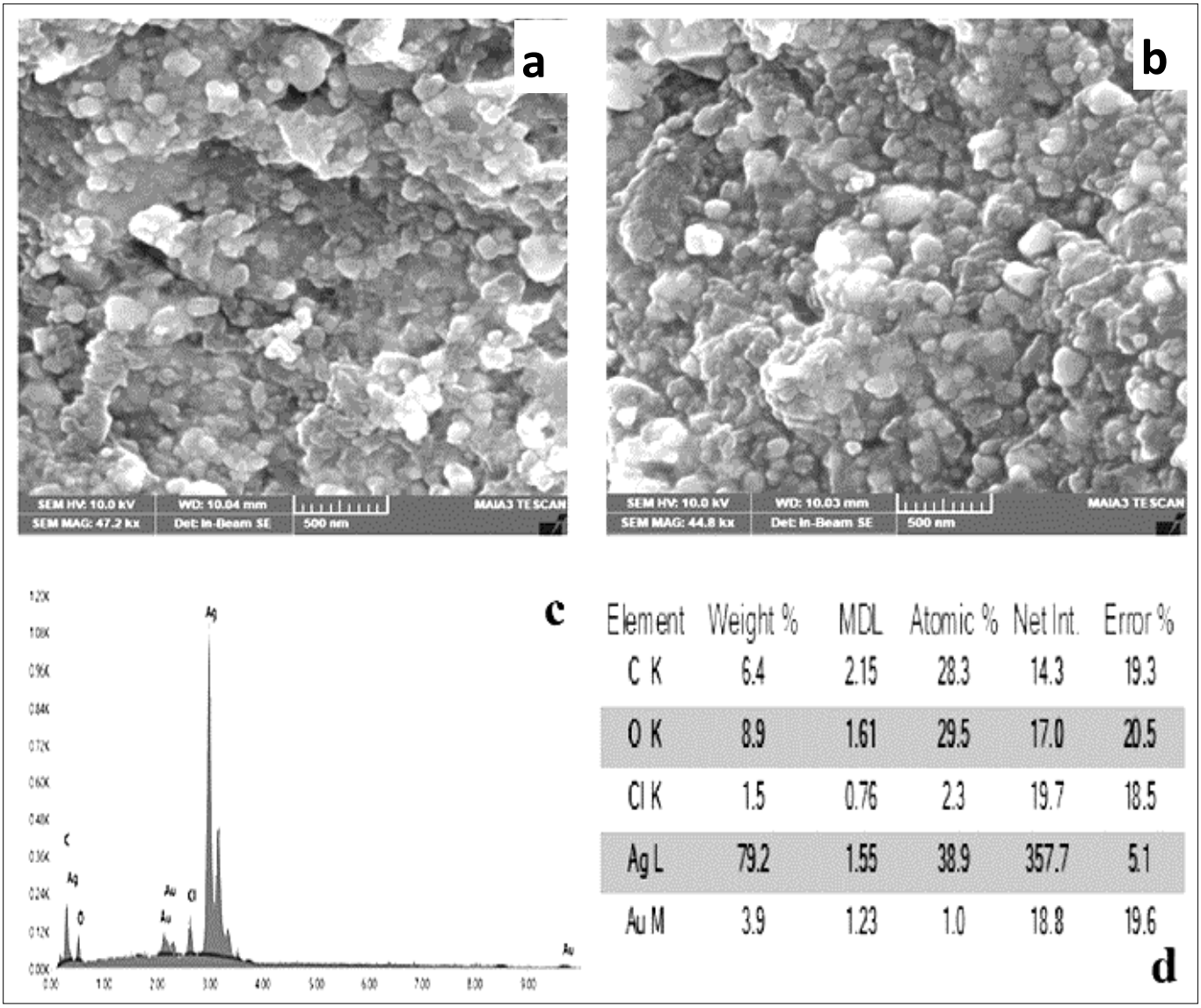


| Element | Weight % | MDL | Atomic % | Net Int. | Error % |
|---|---|---|---|---|---|
| C K | 6.4 | 2.15 | 28.3 | 14.3 | 19.3 |
| O K | 8.9 | 1.61 | 29.5 | 17.0 | 20.5 |
| Cl K | 1.5 | 0.76 | 2.3 | 19.7 | 18.5 |
| Ag L | 79.2 | 1.55 | 38.9 | 357.7 | 5.1 |
| Au M | 3.9 | 1.23 | 1.0 | 18.8 | 19.6 |

d

**Fig. 4.** (a & b) SEM micrograph showing spherical AgNPs with the size of 40 nm and100 k× magnification; (c) EDX spectrum shows strong peak of silver metal; (d) percentage of elements.

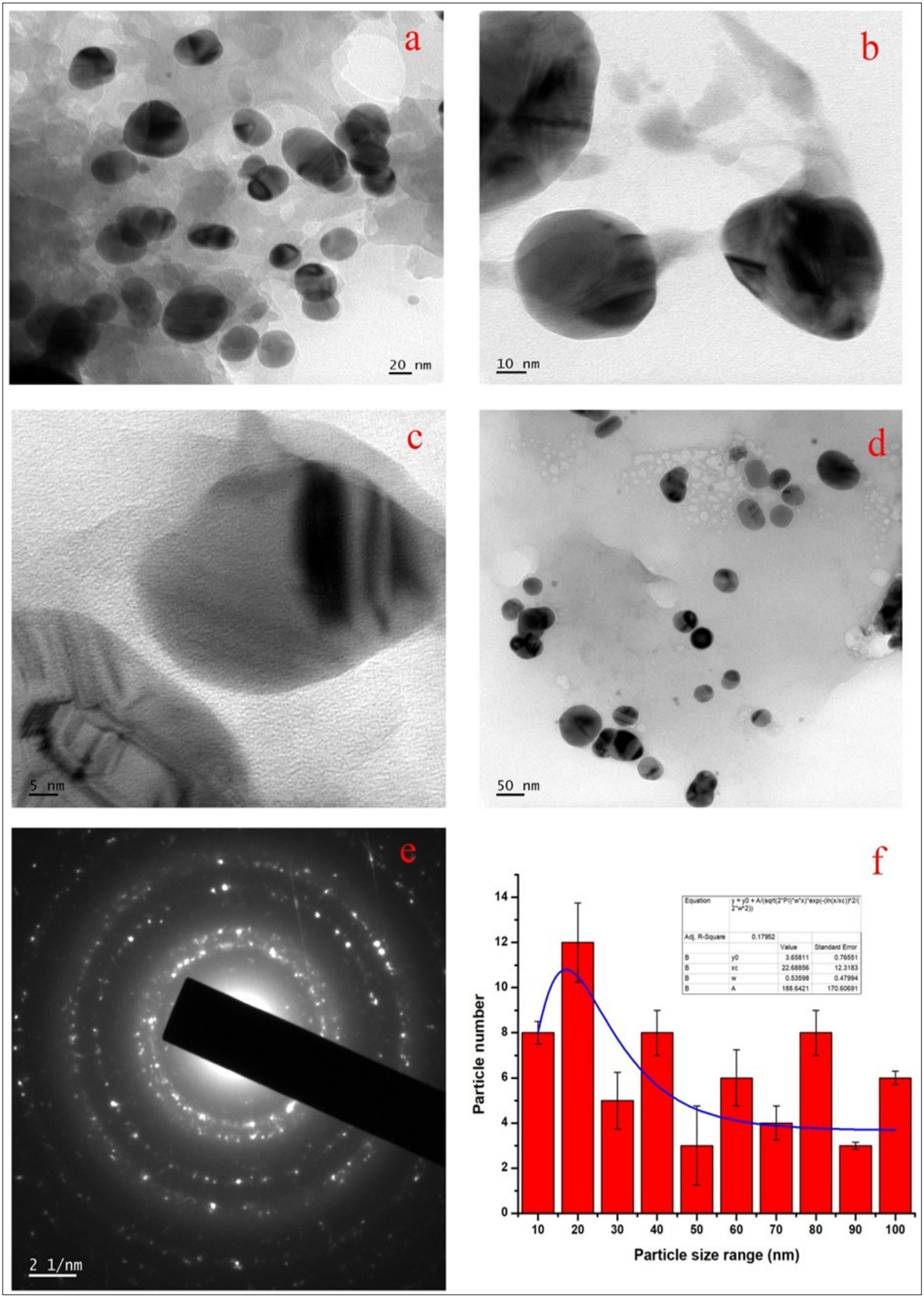


**Fig. 5.** TEM micrograph showing size of AgNPs with SAED pattern with different magnification.

the enhanced stability of the AgNPs due to the capping effect of organic constituents (38). Selected area electron diffraction (SAED) patterns confirmed the presence of elemental AgNPs with a low polydispersity index (PDI), indicating a monodisperse in nature. SAED helps to understand the arrangement of atoms within the nanoparticles and their crystallinity, which affects their properties during the application. The SAED pattern further confirmed the presence of elemental AgNPs.

## Antioxidant activity

Numerous methods are available to evaluate the antioxidant activity. *In vitro* antioxidant screening typically employs several assays, like DPPH, $H_2O_2$ scavenging assay, NO scavenging assay and reducing power activities. Due to the complexity of oxidative processes, the assessment of total antioxidant activity of an antioxidant substance cannot be evaluated by using a single method alone. Therefore, to evaluate the total antioxidant activity at least two methods should be employed (39). The present study was undertaken to demonstrate the antioxidant capacity of the AgNPs synthesized using the extract by four different *in vitro* methods.

## DPPH assay

The antioxidant activity of biosynthesized AgNPs was evaluated using the DPPH assay, which measures the reduction of DPPH through spectrophotometric analysis of the colour change (3). The results demonstrate that both AgNPs and BHT) exhibit antioxidant activity. Notably, AgNPs exhibited 79.5 % antioxidant activity while BHT has 75 % antioxidant activity at 100 µg/mL (Fig. 6a). DPPH scavenging activity of AgNPs increased, based on the reduction of DPPH through electron or hydrogen donation in the reaction solution. At 79.5 % scavenging activity, AgNPs exhibited significant inhibition, evident from the colour change upon adding AgNPs to the DPPH solution. As the AgNPs concentration increased from 10 µg/mL to 100 µg/mL, absorbance at 517 nm decreased; it generally indicates an increase in antioxidant activity. This is because of the decrease in absorbance at 517 nm. DPPH assay suggests that the nanoparticles were scavenging free radicals, which are responsible for the colour change of DPPH at that wavelength.

## $H_2O_2$ scavenging assay

The effect of AgNPs by measuring their ability to neutralize $H_2O_2$, a reactive oxygen species is illustrated in Fig. 6b. Notably, AgNPs exhibited 83.2 % $H_2O_2$ scavenging activity while the standard ascorbic acid showed 80 % $H_2O_2$ scavenging activity at 100 µg/mL. This enhanced activity is attributed to the size and crystalline nature of AgNPs. This result proved that AgNPs have strong $H_2O_2$ scavenging activity, which is comparable with that of ascorbic acid. The free radical scavenging activity is likely due to the presence of phyto compounds, especially flavonol, glycosides and phloroglucinols, which donate the hydrogen atoms in their OH groups (40). This result proved that a higher percentage of $H_2O_2$ scavenging indicates a greater antioxidant capacity of the AgNPs.

## NO scavenging assay

NO is an important bioregulatory molecule required for many biological processes and acts as a signaling molecule with multiple biological functions in plants. The NO scavenging activity of biosynthesized AgNPs was evaluated and compared with that of standard BHT. The NO scavenging activity of AgNPs was found to be concentration dependent, which increased steadily from 10 µg/mL to 100 µg/mL. The AgNPs have 72 % NO scavenging activity while standard BHT showed 80 % at a higher concentration of 100 µg/mL (Fig. 6c). The results indicate that BHT has greater NO scavenging activity than AgNPs. The observed difference can be explained by the interaction of AgNPs with NO radicals, which are characterized by their high unstable and electronegativity and allowing them to accept electrons. This interaction can involve the AgNPs acting as electron donors, reacting with the NO radicals to form less reactive species from the AgNPs (42).

## Ferric reducing power assay

The reducing power of biosynthesized AgNPs derived from plant extracts was found to be concentration dependent, which increased correspondingly with increasing AgNPs concentration. Since the concentration of AgNPs was increased from 10 µg/mL to 100 µg/mL, the reducing power also increased from 15 % to 71 %, whereas standard BHT exhibited 81.5 % reducing power (Fig. 6d). The reducing power of AgNPs may serve as a significant indicator of their potential antioxidant activity (23). So, the present assay shows the presence of antioxidants in *in vitro* raised *H. wightianum* extract, which reduced the ferricyanide/$Fe^{3+}$ complex to its ferrous form. The reducing power increased with the concentration of phyto compounds, especially flavonol glycosides and phloroglucinols and other chemical constituents of the extract. Generally, the antioxidant potential of AgNPs depends on the chemical moieties present in the extract. If the plant extract is rich in flavonoids and phenolic compounds, the NPs showed high scavenging activity (3). The free O-H group on the aromatic ring is responsible for the antioxidant properties. The hydrogen of O-H on the aromatic ring was donated to the free radical, resulting in the stability of the free radical species. (14). These results confirmed the antioxidant abilities of AgNPs and agree with previously studied plant-based AgNPs (10). Notably, the reducing powers of AgNPs also increased with increasing concentrations. These results indicate that biosynthesized AgNPs can react with free radicals to convert them into stable, non-reactive species and to terminate radical chain reactions (43).

## Antibacterial activity

The biosynthesized AgNPs exhibited notable antibacterial activity against selected bacteria (Fig. 7a-d). Specifically, the antibacterial activity of AgNPs was found to depend on the bacterial species and AgNPs showed minimal activity against *E .coli* with a zone of inhibition 5 mm and no activity against some other bacteria. AgNPs demonstrated higher antibacterial activity against *P. aeruginosa* (Gram-negative) and *S. aureus* (Gram-positive) with a zone of inhibition 14 mm and 15 mm, respectively as shown in Fig. 7b & c. This disparity is likely due to differences in cell wall structure between Gram-positive and Gram-negative bacteria. The significant bactericidal effect observed can be attributed to the release of silver cations from AgNPs, which serve as a source of the $Ag^+$ bactericidal agent (44). AgNPs penetration into bacterial cell walls leads to inactivating cellular proteins and enzymes, generating $H_2O_2$ and ultimately leading to bacterial cell death (45, 46). AgNPs are widely used as antimicrobial agents in

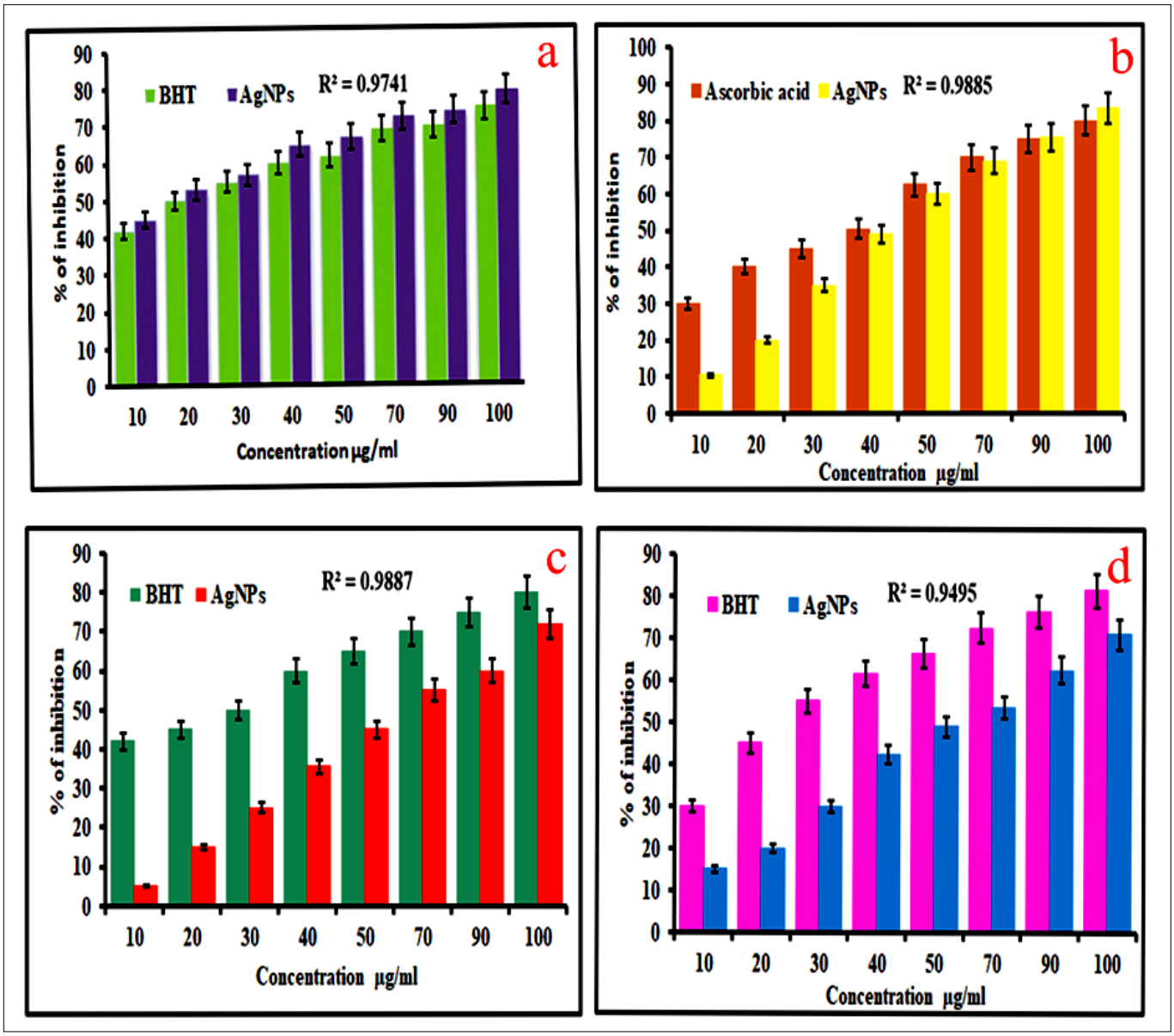


**Fig. 6.** Antioxidant activity of biosynthesized AgNPs from *in vitro* raised plant extracts. (a): DPPH; (b): $H_2O_2$ scavenging activity; (c): NO scavenging assay; (d): Ferric reducing power assay.

wound dressings, catheters, the food industry and other medical devices. They are effective against a broad spectrum of bacteria, fungi and viruses. In the food industry, microbial contamination is one of the main problems of food, resulting in spoilage and foodborne diseases. AgNPs were used to extend shelf life and prevent microbial growth. (47). Therefore, AgNPs can be utilized in the food industry to inhibit food spoilage, enhancing food quality assurance systems throughout the production processes (48). Besides, it may be used in medical instruments and food packaging (49). Notably, biologically synthesized AgNPs using various plant extracts have demonstrated similar potent bactericidal activity (13, 50, 51).

## Ecotoxicity studies

The ecotoxicity of AgNPs to *A. salina* and nauplii after 12 to72 hr exposure were studied and results are shown in Fig. 8. After 24 hr of exposure, no mortality was observed in treatments and controls, whereas 72 hr exposure resulted in increased mortality rates, ranging from 15 - 35.23 % for nauplii and 14 - 30 % for adults. Mortality rates were significantly higher at high exposure time, with nauplii exhibiting 30.27 - 69 % mortality and adults showing 25.34 - 65 % mortality. At 6 hr, NPs treatment exhibited 0 - 4 % and 0 - 5 % mortality rates in adult and nauplii respectively, with controls not affected. From the results, the mortality rate was dose and time (12 to 72 hr) dependent in the range of 20 µg/mL to 150 µg/mL in nauplii and adults. As shown in Fig. 9, both nauplii and adult *A. salina* exhibited almost the same levels of momentum and exposure time-dependent mortality, when exposed to different concentrations of AgNPs (20 -150 µg/mL) for different periods of exposure (6 - 72 hr). When exposed for 72 hr, the mortality was below 30 % at 20 µg/mL and about 70 % at 150 µg/mL. No mortality was observed when exposed for only 6 hr. The adult mortality rate was less than nauplii. The nauplii mortality rate rose from zero at 20 µg/mL to 5 % at 150 µg/mL for 12 hr of exposure. This suggests that the binary compound AgNPs suspensions did not cause an acute toxic effect in nauplii, even at high concentrations of 80 µg/mL within an hour after 24 hr of exposure. AgNPs were not toxic to the adult and nauplii at optimum concentration and long exposure times (52). The $LC_{50}$ values for nauplii were 447.30 µg/mL at 24 hr and 101.94 µg/mL at 72 hr, while adult $LC_{50}$ values were 480.6 µg/mL at 24 hr and 100 µg/mL at 72 hr. $LC_{50}$ rates

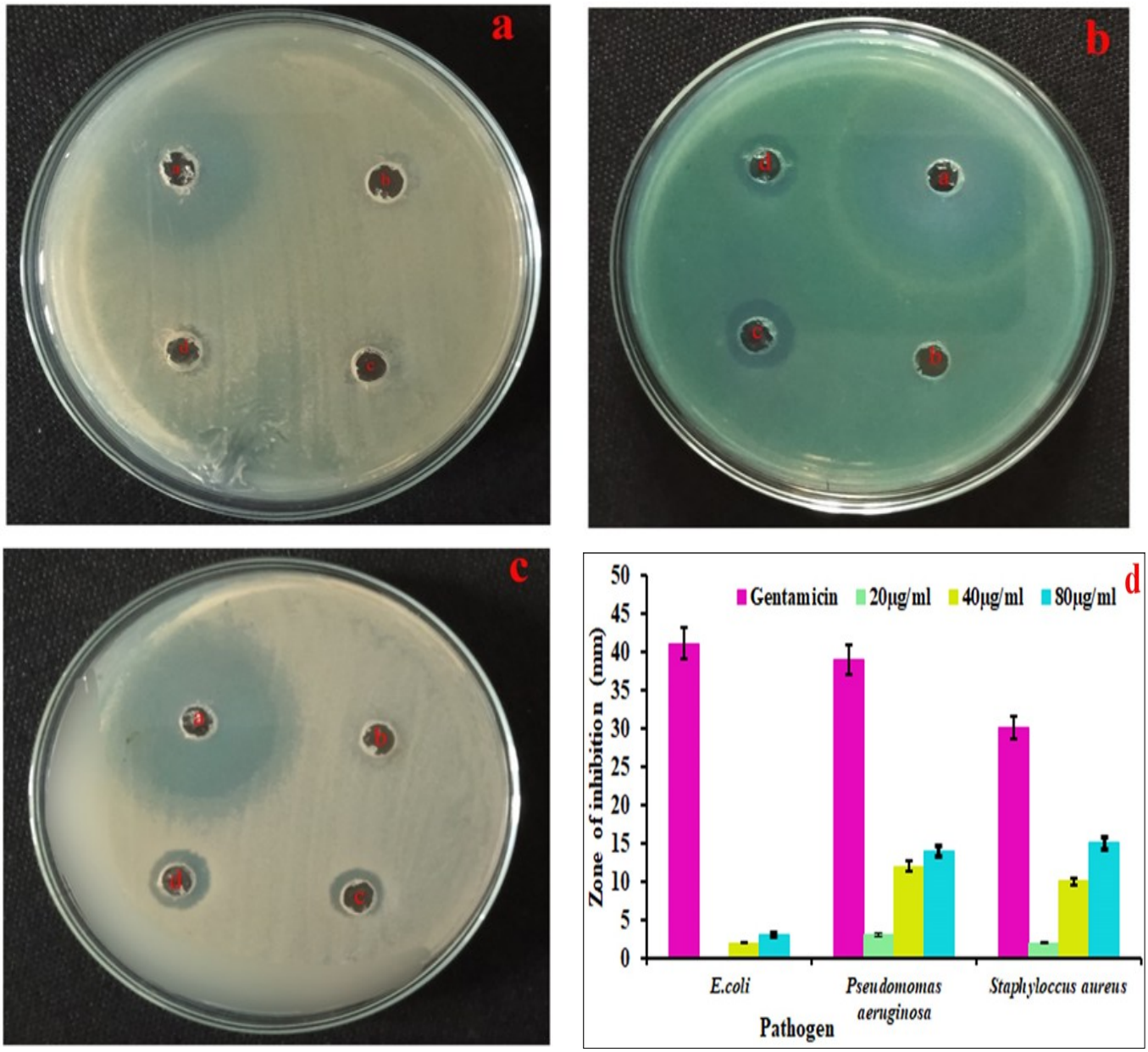


**Fig. 7.** Antimicrobial activity of synthesized AgNPs against various pathogenic bacterial strains with different concentrations (40 and 80 µg/mL, standard antibiotic).

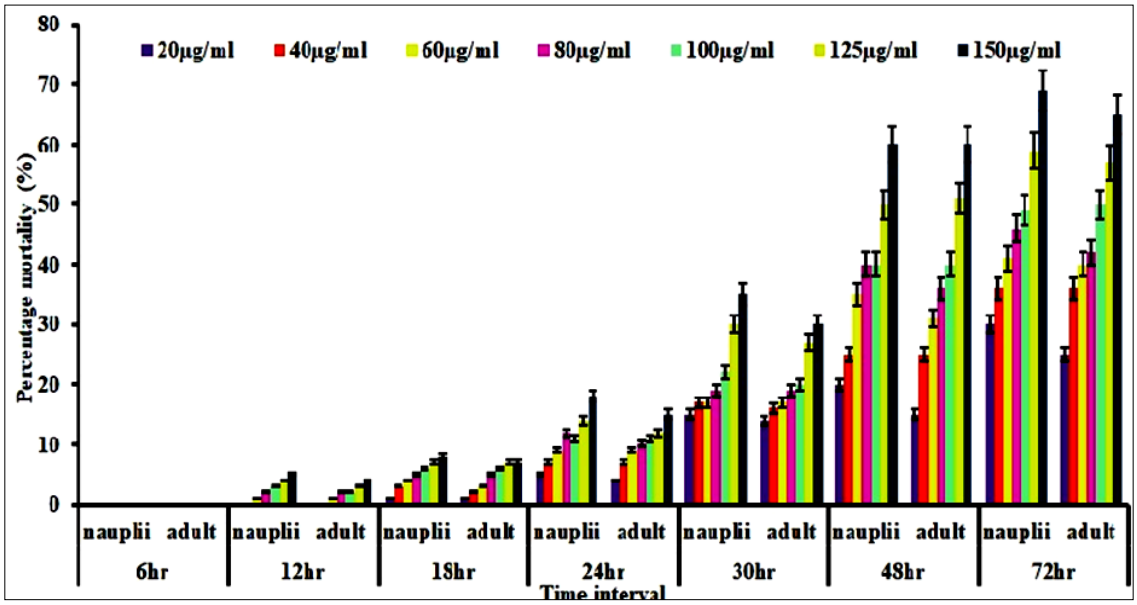


**Fig. 8.** Percent mortality rates for *Artemia* nauplii measured for up to 72 hr exposure to different concentration of colloidal biosynthesized AgNPs.

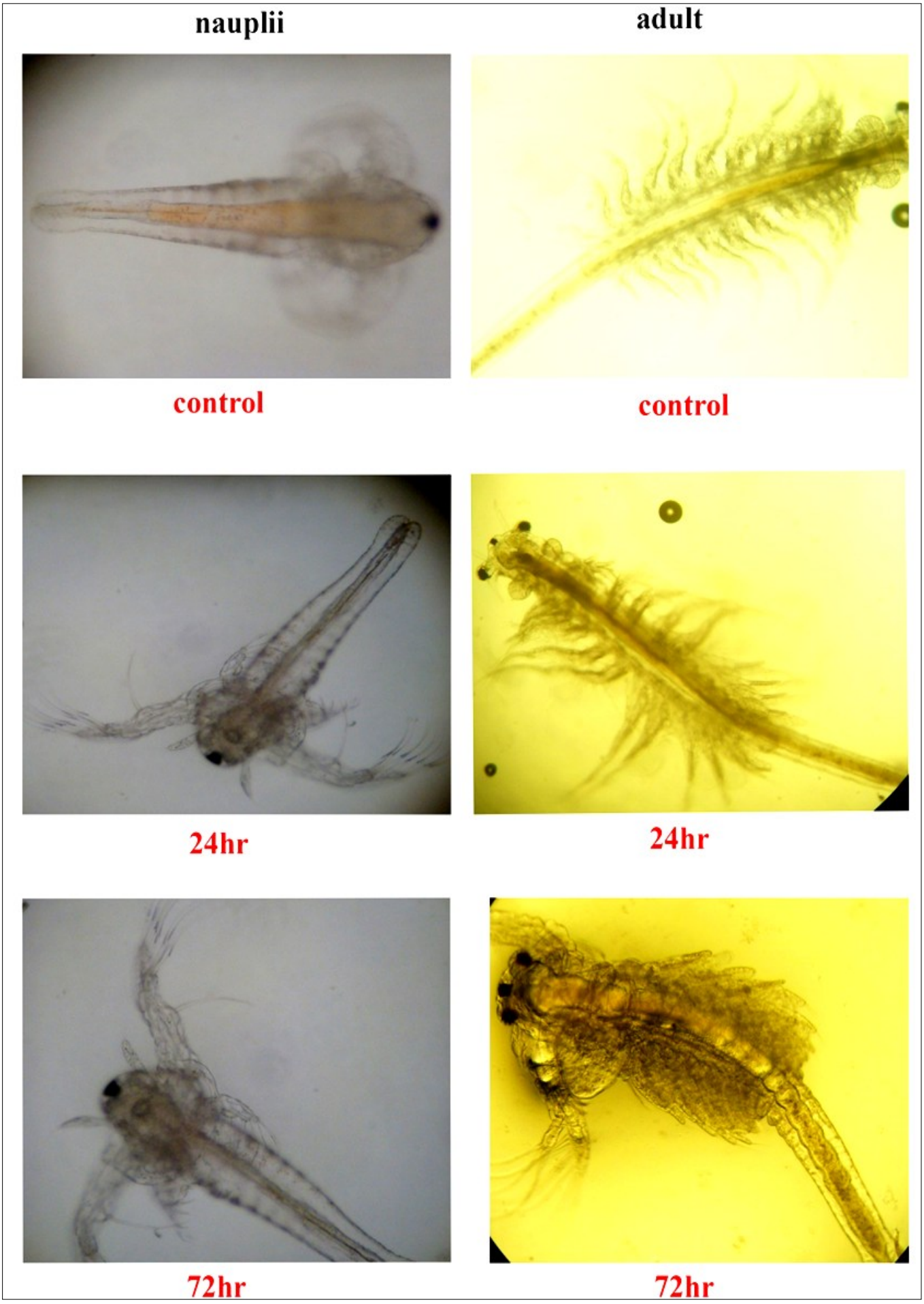


**Fig. 9.** Accumulation of AgNPs in *Artemia* adult and nauplii at 24 hr and 72 hr exposure.

were varied according to exposure time and AgNPs concentration during the experiment. Based on the $LC_{50}$ value, these findings suggest that AgNPs colloidal suspensions are toxic to nauplii and adults at elevated levels, with prolonged exposure increasing mortality risk (21). The low acute toxicity effect was also observed on nauplii (53). AgNPs reduced toxicity may be attributed to size and surface area reduction due to agglomeration in colloidal conditions and inside *Artemia* guts (54). Our result implies that prolonged exposure at 72 hr increases the mortality risk of *Artemia* nauplii and adults. The uptake of nanoparticles by *Artemia* is influenced by the NPs concentration and exposure time, while the size of the NPs was not a major factor (55).

## Conclusion

In this study, we have effectively synthesized AgNPs using the *in vitro* plant extract of *H. wightianum* using simple technique of biosynthesis. Secondary metabolites in plant extracts are good reducing and capping agents for the green synthesis of AgNPs. The green synthesized AgNPs have been used in a wide range of pharmaceutical and medical applications because of their antibacterial and antioxidant properties. FE-SEM and TEM analysis revealed the crystalline nature of biosynthesized AgNPs with an average particle size of 16.47 nm. The antibacterial potential was high for the *in vitro* based plant extract-capped AgNPs against Gram-negative rather than Gram-positive bacteria. Moreover, the free radical scavenging ability of these nanoparticles was remarkable; *Artemia* showed only mortality at 72 hr of exposure to AgNPs. These results concluded that the colloidal AgNPs were nontoxic to *Artemia*. The green synthesis approaches have been suggested as economical alternatives to the physical and chemical nano-synthesis techniques. Hence, this approach holds potential evidence for the large-scale production of AgNPs developed from plant extract in food packaging. The antibacterial activity assays and antioxidant assay result ensures the usage in the pharmaceutical industries and might be of value for many biotechnological and medicinal applications. Further studies will focus on AgNPs pharmacological applications.

## Acknowledgements

The authors are thankful to the Head, Department of Botany, University of Kerala, India, for providing the facility for doing this work. The one of the authors Neethu Vijayakumar is thankful to the CSIR, New Delhi, India for providing financial support through Senior Research Fellow (Ref: File No.08/538(0005)/2017-EMR-1). The authors thank Director, Central Laboratory for Instrumentation and Facilitation (CLIF), University of Kerala for providing XRD, FTIR analysis. The authors are grateful to SAIF, Calicut University, for providing FE-SEM-EDX and TEM analysis.

## Authors' contributions

NV was responsible for the study design, sample collection, experiment execution, data analysis and manuscript preparation. SVR, AG and MS critically revised the article for significant intellectual content, edited the manuscript and approved it. All authors reviewed and approved the final version of the manuscript.

## Compliance with ethical standards

**Conflict of interest:** The authors declare that they have no competing interests.

**Ethical issues:** None

## References

1. Panda MK, Dhal NK, Kumar M, Mishra PM, Behera RK. Green synthesis of silver nanoparticles and its potential effect on phytopathogens. Mater Today Proc. 2021;35(2):233–38. https://doi.org/10.1016/j.matpr.2020.05.188
2. Liu R, Luo C, Pang Z, Zhang J, Ruan S, Wu M, et al. Advances of nanoparticles as drug delivery systems for disease diagnosis and treatment. Chin Chem Lett. 2023;34(2):107518. https://doi.org/10.1016/j.cclet.2022.05.032
3. Bhakya S, Muthukrishnan S, Sukumaran M, Grijalva M, Cumbal L, Benjamin JHF, et al. Antimicrobial, antioxidant and anticancer activity of biogenic silver nanoparticles–an experimental report. RSC Adv. 2016;84(6):81436–46. https://doi.org/10.1039/C6RA17569D
4. Muthukrishnan S, Kumar TS, Rao MV. Anticancer activity of biogenic nanosilver and its toxicity assessment on *Artemia salina* - evaluation of mortality, accumulation and elimination: an experimental report. J Environ Chem Eng. 2017;5(2):1685–95. https://doi.org/10.1016/j.jece.2017.03.004
5. Singh RP, Handa R, Manchanda G. Nanoparticles in sustainable agriculture: an emerging opportunity. J Control Release. 2021;329:1234–48. https://doi.org/10.1016/j.jconrel.2020.10.051
6. Liu B, Zhuang J, Wei G. Recent advances in the design of colorimetric sensors for environmental monitoring. Environ Sci Nano. 2020;7(8):2195–213. https://doi.org/10.1039/D0EN00449A
7. Taha TB, Barzinjy AA, Hussain FHS, Nurtayeva T. Nanotechnology and computer science: trends and advances. Memor Mater Devices Circuits Syst. 2022;2:100011. https://doi.org/10.1016/j.memori.2022.100011
8. Wei Y, Yan B. Nano products in daily life: to know what we do not know. Natl Sci Rev. 2016;3(4):414–15. https://doi.org/10.1093/nsr/nww073
9. Boopathi S, Davim JP. Applications of nanoparticles in various manufacturing processes. In: Sustainable Utilization of Nanoparticles and Nanofluids in Engineering Applications. IGI Global; 2023. p. 1–31 https://doi.org/10.4018/978-1-6684-9135-5.ch001
10. Zahoor M, Nazir N, Iftikhar M, Naz S, Zekker I, Burlakovs J, et al. A review on silver nanoparticles: classification, various methods of synthesis and their potential roles in biomedical applications and water treatment. Water. 2021;13(16):2216. https://doi.org/10.3390/w13162216
11. Abed MS, Jawad ZA. Nanotechnology for defence applications. In: Mubarak NM, Gopi S, Balakrishnan P, editors. Nanotechnology for Electronic Applications. Materials Horizons: From Nature to Nanomaterials. Singapore: Springer; 2022. p. 187–205 https://doi.org/10.1007/978-981-16-6022-1_10
12. Muthukrishnan S, Bhakya S, Kumar TS, Rao MV. Biosynthesis, characterization and antibacterial effect of plant-mediated silver nanoparticles using *Ceropegia thwaitesii*–an endemic species. Ind Crops Prod. 2015;63:119–24. https://doi.org/10.1016/j.indcrop.2014.10.022
13. Sreelekshmi R, Siril EA, Muthukrishnan S. Role of biogenic silver nanoparticles on hyperhydricity reversion in *Dianthus chinensis* L. an *in vitro* model culture. J Plant Growth Regul. 2022;41:23–39.

https://doi.org/10.1007/s00344-020-10276-0

14. Kumar VK, Muthukrishnan S, Rajalakshmi R. Phytostimulatory effect of phytochemical fabricated nanosilver (AgNPs) on *Psophocarpus tetragonolobus* (L.) DC. seed germination: an insight from antioxidative enzyme activities and genetic similarity studies. Curr Plant Biology. 2020;23:100158. https://doi.org/10.1016/j.cpb.2020.100158
15. Nunes BS, Carvalho FD, Guilhermino LM, Van Stappen G. Use of the genus *Artemia* in ecotoxicity testing. Environ Pollut. 2006;144(2):453–62. https://doi.org/10.1016/j.envpol.2005.12.037
16. Rekka E, Kourounakis PN. Effect of hydroxyethyl rutosides and related compounds on lipid peroxidation and free radical scavenging activity. some structural aspects. J Pharm Pharmacol. 1991;43(7):486–91. https://doi.org/10.1111/j.2042-7158.1991.tb03519.x
17. Asada K. Ascorbate peroxidase–a hydrogen peroxide-scavenging enzyme in plants. Physiol Plant. 1992;85(2):235–41. https://doi.org/10.1111/j.1399-3054.1992.tb04728.x
18. Marcocci L, Maguire JJ, Droylefaix MT, Packer L. The nitric oxide-scavenging properties of *Ginkgo biloba* extract EGb 761. Biochem Biophys Res Commun. 1994;201(2):748–55. https://doi.org/10.1006/bbrc.1994.1764
19. Corzo A, Niell FX. Determination of nitrate reductase activity in *Ulva rigida* C. Agardh by the *in-situ* method. J Exp Mar Biol Ecol. 1991;146(2):181–91. https://doi.org/10.1016/0022-0981(91)90024-Q
20. Sen A, Batra A. Evaluation of antimicrobial activity of different solvent extracts of medicinal plant: *Melia azedarach* L. Int J Curr Pharm Res. 2012;4(2):67–73.
21. Ates M, Daniels J, Arslan Z, Farah IO. Effects of aqueous suspensions of titanium dioxide nanoparticles on *Artemia salina*: assessment of nanoparticle aggregation, accumulation and toxicity. Environ Monit Assess 2013;185:3339–48. https://doi.org/10.1007/s10661-012-2794-7
22. Cimino MC. New OECD genetic toxicology guidelines and interpretation of results. In: Genetic toxicology and cancer risk assessment. CRC Press; 2001. pp. 237–62
23. Jiang H, Moon KS, Zhang Z, Pothukuchi S, Wong CP. Variable frequency microwave synthesis of silver nanoparticles. J Nanopart Res. 2006;8:117–24. https://doi.org/10.1007/s11051-005-7522-6
24. Ahmad A, Mukherjee P, Senapati S, Mandal D, Khan MI, Kumar R, et al. Extracellular biosynthesis of silver nanoparticles using the fungus *Fusarium oxysporum*. Colloids Surf B Biointerfaces. 2003;28(4):313–18. https://doi.org/10.1016/S0927-7765(02)00174-1
25. Kelly KL, Coronado E, Zhao LL, Schatz GC. The optical properties of metal nanoparticles: the influence of size, shape and dielectric environment. J Phys Chem B. 2003;107(3):668–77. https://doi.org/10.1021/jp026731y
26. Bi S, Song D, Tian Y, Zhou X, Liu Z, Zhang H. Molecular spectroscopic study on the interaction of tetracyclines with serum albumins. Spectrochim Acta A Mol Biomol Spectrosc. 2005;61(4):629–36. https://doi.org/10.1016/j.saa.2004.05.028
27. Kowshik M, Deshmukh N, Vogel W, Urban J, Kulkarni SK, Paknikar KM. Microbial synthesis of semiconductor CdS nanoparticles, their characterization and their use in the fabrication of an ideal diode. Biotechnol Bioeng. 2002;78(5):583–88. https://doi.org/10.1002/bit.10233
28. Mata R, Nakkala JR, Sadras SR. Biogenic silver nanoparticles from *Abutilon indicum*: their antioxidant, antibacterial and cytotoxic effects *in vitro*. Colloids Surf B Biointerfaces. 2015;128:276–86. https://doi.org/10.1016/j.colsurfb.2015.01.052
29. Kasthuri J, Veerapandian S, Rajendiran N. Biological synthesis of silver and gold nanoparticles using apiin as reducing agent. Colloids Surf B Biointerfaces. 2009;68(1):55–60. https://doi.org/10.1016/j.colsurfb.2008.09.021
30. Fayaz AM, Balaji K, Girilal M, Yadav R, Kalaichelvan PT, Venketesan R. Biogenic synthesis of silver nanoparticles and their synergistic effect with antibiotics: a study against gram-positive and gram-negative bacteria. Nanomedicine. 2010;6(1):103–09. https://doi.org/10.1016/j.nano.2009.04.006
31. Feng N, Guo X, Liang S. Adsorption study of copper (II) by chemically modified orange peel. J Hazard Mater. 2009;164(2-3):1286–92. https://doi.org/10.1016/j.jhazmat.2008.09.096
32. Qiu L, Liu F, Zhao L, Yang W, Yao J. Evidence of a unique electron donor – acceptor property for platinum nanoparticles as studied by XPS. Langmuir. 2006;22(10):4480–82. https://doi.org/10.1021/la053071q
33. Bouhajeb R, Abreu AC, Fernández S, Bayrem-Ghedira M, Chekir-Ghedira L, Fernández I, et.al. Green synthesis of highly monodisperse and spherical Ag nanoparticles by a combination of *Teucrium ramosissimum* Desf. (Lamiaceae) extracts with emphasis on the stabilizing and capping biomolecules.ACS Sustainable Chem Eng. 2024;12(10):4132–45. https://doi.org/10.1021/acssuschemeng.3c07504
34. Safa MAT, Koohestani H. Green synthesis of silver nanoparticles with green tea extract from silver recycling of radiographic films. Results Eng. 2024;21:101808. https://doi.org/10.1016/j.rineng.2024.101808
35. Zulfiqar Z, Khan RRM, Summer M, Saeed Z, Pervaiz M, Rasheed S, et al. Plant-mediated green synthesis of silver nanoparticles: synthesis, characterization, biological applications and toxicological considerations: a review. Biocatal Agric Biotechnol. 2024;57:103121. https://doi.org/10.1016/j.bcab.2024.103121
36. Ibrahim NH, Taha GM, Hagaggi NSA, Moghazy MA. Green synthesis of silver nanoparticles and its environmental sensor ability to some heavy metals. BMC Chem. 2024;18:7. https://doi.org/10.1186/s13065-023-01105-y
37. Velmurugan G, Chohan JS, Kannan VS, Paramasivam P, Shankar VS, Maranan R. Green synthesis of silver nanoparticles from southern *Eucalyptus globulus*: potent antioxidants and photocatalysts for rhodamine B dye degradation. Desalin Water Treat. 2024;320:100687. https://doi.org/10.1016/j.dwt.2024.100687
38. Padalia H, Moteriya P, Chanda S. Green synthesis of silver nanoparticles from marigold flower and its synergistic antimicrobial potential. Arab J Chem. 2015;8(5):732–41. https://doi.org/10.1016/j.arabjc.2014.11.015
39. GÜLÇin I, Alici HA, Cesur M. Determination of *in vitro* antioxidant and radical scavenging activities of propofol. Chem Pharm Bull. 2005;53(3):281–85. https://doi.org/10.1248/cpb.53.281
40. Sagbo IJ, Afolayan AJ, Bradley G. Antioxidant, antibacterial and phytochemical properties of two medicinal plants against the wound infecting bacteria. Asian Pac J Trop Biomed. 2017;7(9):817–25. https://doi.org/10.1016/j.apjtb.2017.08.009
41. Boora F, Chirisa E, Mukanganyama S. Evaluation of nitrite radical scavenging properties of selected Zimbabwean plant extracts and their phytoconstituents. J Food Process. 2014;918018:7p. https://doi.org/10.1155/2014/918018
42. Subramanian R, Subbramaniyan P, Raj V. Antioxidant activity of the stem bark of *Shorea roxburghii* and its silver reducing power. SpringerPlus. 2013;2:28. https://doi.org/10.1186/2193-1801-2-28
43. Paszek MJ, DuFort CC, Rubashkin MG, Davidson MW, Thorn KS, Liphardt JT, et al. Scanning angle interference microscopy reveals cell dynamics at the nanoscale. Nat methods. 2012;9:825–27. https://doi.org/10.1038/nmeth.2077
44. Raffi M, Hussain F, Bhatti TM, Akhter JI, Hameed A, Hasan MM. Antibacterial characterization of silver nanoparticles against *E. coli* ATCC-15224. J Mater Sci Technol. 2008;24(2):192–96.
45. Kokkoris M, Trapalis CC, Kossionides S, Vlastou R, Nsouli B, Grötzschel R, et al. RBS and HIRBS studies of nanostructured $AgSiO_2$ sol-gel thin coatings. Nuclear Nucl Instrum Methods Phys Res B. 2002;188(1–4):67–72. https://doi.org/10.1016/S0168-583X(01)01020-5

46. Carbone M, Donia DT, Sabbatella G, Antiochia R. Silver nanoparticles in polymeric matrices for fresh food packaging. J King Saud Univ Sci. 2016;28(4):273–79. https://doi.org/10.1016/j.jksus.2016.05.004

47. Xu L, Wang YY, Huang J, Chen CY, Wang ZX, Xie H. Silver nanoparticles: synthesis, medical applications and biosafety. Theranostics. 2020;10(20):8996–9031. https://doi.org/10.7150/thno.45413

48. Mahdi SS, Vadood R, Nourdahr R. Study on the antimicrobial effect of nanosilver tray packaging of minced beef at refrigerator temperature. Glob Vet. 2012; 9(3):284–89.

49. Bhakya S, Muthukrishnan S, Sukumaran M, Muthukumar M. Biogenic synthesis of silver nanoparticles and their antioxidant and antibacterial activity. Appl Nanosci. 2016;6:755–66. https://doi.org/10.1007/s13204-015-0473-z

50. Balachandar R, Navaneethan R, Biruntha M, Kumar KKA, Govarthanan M, Karmegam N. Antibacterial activity of silver nanoparticles phytosynthesized from *Glochidion candolleanum* leaves. Mater Lett. 2022;311:131572. https://doi.org/10.1016/j.matlet.2021.131572

51. Palácio SM, de Almeida JCB, de Campos ÉA, Veit MT, Ferreira LK, Deon MTM. Silver nanoparticles effect on *Artemia salina* and *Allium cepa* organisms: influence of test dilution solutions on toxicity and particles aggregation. Ecotoxicology. 2021;30:836–50. https://doi.org/10.1007/s10646-021-02393-7

52. Kamaraj C, Ragavendran C, Manimaran K, Sarvesh S, Islam ARMT, Malafaia G. RETRACTED: Green synthesis of silver nanoparticles from *Cassia auriculata*: targeting antibacterial, antioxidant activity and evaluation of their possible effects on saltwater microcrustacean, *Artemia* nauplii (non-target organism). Sci Total Environ. 2023;861:160575. https://doi.org/10.1016/j.scitotenv.2022.160575

53. Unal İ, Egri S, Ates M. Green Synthesis (*Paeonia kesrouanensis*) of silver nanoparticles and toxicity studies in *Artemia salina*. Bull Environ Contam Toxicol. 2022;109:1150–54. https://doi.org/10.1007/s00128-022-03601-8

54. Sarkheil M, Johari SA, An HJ, Asghari S, Park HS, Sohn EK, et al. Acute toxicity, uptake and elimination of zinc oxide nanoparticles (ZnO NPs) using saltwater microcrustacean, *Artemia franciscana*. Environ Toxicol Pharmacol. 2018;57:181–88. https://doi.org/10.1016/j.etap.2017.12.018

## Additional information

**Peer review**: Publisher thanks Sectional Editor and the other anonymous reviewers for their contribution to the peer review of this work.

**Reprints & permissions information** is available at https://horizonepublishing.com/journals/index.php/PST/open_access_policy

**Publisher's Note**: Horizon e-Publishing Group remains neutral with regard to jurisdictional claims in published maps and institutional affiliations.

**Indexing**: Plant Science Today, published by Horizon e-Publishing Group, is covered by Scopus, Web of Science, BIOSIS Previews, Clarivate Analytics, NAAS, UGC Care, etc
See https://horizonepublishing.com/journals/index.php/PST/indexing_abstracting



**Publisher information:** Plant Science Today is published by HORIZON e-Publishing Group with support from Empirion Publishers Private Limited, Thiruvananthapuram, India.